doi:10.1038/nature12059

1: Supplementary Text

1.1 Size effects

Estimated body masses for our study taxa encompass six orders of magnitude (average estimates range from <1 kg to >10,000 kg, see Table S4). The potential for significant allometric changes of CoM position as well as (or instead of) evolutionary changes in our sample is therefore substantial. To investigate this, we analysed correlations (Pearson's; see Methods Summary in main text) between estimated body mass (log-transformed) and estimated craniocaudal CoM (normalised to body mass$^{1/3}$). A significant negative correlation (Pearson's, $p<0.01$, $R = -0.71$) was found.

Given that previously identified evolutionary trends towards large body size in Tetanurae/basal Coelurosauria and reduced body size in derived Maniraptora (e.g. [31]) are also recovered here (see Supplementary Table S6), it is possible that cranial shifts in whole-body CoM towards the avian terminus of the bird-line are a result of allometric shifts associated with reduced body size. Conversely, it is possible that concurrence of size reduction with the morphological trends noted above is the cause of a negative correlation between size and CoM position. The addition of more early bird-line small-bodied taxa would enable this to be tested.

1.2: Evolutionary Trends in Morphological Evolution

There are two phylogenetic transitions along the bird-line in which our analysis infers that a rapid series of correlated morphological changes occurred, and which were omitted from the main text as they could not be definitely associated with changes in CoM position. First,

between basal Theropoda and basal Neotheropoda (nodes 5-6, Fig. 4), there seems to have been a rapid increase in relative head mass (Fig. 4.1) and relative neck mass (Fig. 4.2). Visual inspection of the digitised fossil material indicates that this is related mainly to an elongation (rather than a thickening) of the neck and enlargement of the skull from basal dinosauromorphs to later theropods. That this has no unambiguous correlation with CoM position around this transition is interesting, particularly as there are large discontinuities in the mass of the tail and the caudofemoral muscle between the same nodes (Fig. 5). However, the envelope of values indicated by our sensitivity analysis is at its widest between nodes 5 and 7, suggesting a high degree of uncertainty when it comes to reconstruction of basal neotheropod body proportions - with additional specimens, it may be that a corresponding discontinuity in CoM *is* found to be present, but this is not rigorously supported by our current analysis.

This is particularly noteworthy given a previous study of a remarkable series of footprints, attributed to early theropods that were fossilised in deep enough mud to preserve some indications of metatarsal angle[32]. These indicated that the metatarsus was held at quite a high angle of plantarflexion, close to the substrate, at least early in the stance phase, rather than in a more vertical position as has been postulated to be the ancestral condition for bipedal dinosaurs. A more plantarflexed metatarsus could have placed the foot directly underneath a cranially positioned CoM without requiring a flexed hip or cranially inclined femur (a different form of 'crouched' posture to that of Neornithes), but because the GRF would then have passed cranial to the knee joint, this would indicate that mid-stance limb support involved flexion (rather than extension) musculature at the knee. This is highly speculative, and given how unlike the limb support mechanics of living birds it is, not well supported.

However, the implication that there is something unusual about early theropod terrestrial locomotion that does not necessarily fit into a simple pattern of gradually increasing limb flexion on the line to Neornithes is interesting. Further biomechanical analysis of basal neotheropod anatomy and trackways may produce some novel insights into theropod locomotor evolution as a whole.

The second phylogenetic transition at which several major associated morphological trends seem to have occurred is between basal Ornithurae and extant Neornithes (nodes 15-16, Fig. 4). This transition was associated with sharp decreases in relative head mass (Fig. 4a), relative neck mass (Fig. 4b), relative trunk mass (Fig. 4c), and a major increase in pelvic limb mass (Fig. 4e). The raw data (see Table S4) confirm that this reflects real proportional differences between the neornithine (*Gallus*; a junglefowl close to the ancestral wild-type) and the basal ornithurine (*Yixianornis*) - when normalised to body mass, the head and neck of *Gallus* are lighter by ~0.03 body mass, the trunk lighter by 0.1 body mass, and the pelvic limb heavier by 0.08 body mass. However, this transition also involves the longest temporal distance between bird-line phylogenetic nodes in our analysis (122 Ma, see Table S2), and so this already considerable difference may be exacerbated. Further analyses including a wider range of extant Neornithes (Palaeognathae and Galloanserae) as well as more basal Ornithurae (e.g. *Apsaravis*, basal Hesperornithiformes, *Ichthyornis*) are needed to test the validity of these morphological trends.

1.3: Investigation of Potential Phylogenetic Biases

To assess the influence of phylogeny on the regression analyses we used to test the influence of individual segment masses on CoM position, phylogenetic independent contrasts (PIC)

analysis was carried out using the PDAP module[33] for Mesquite 2.75[34] and the REGRESSION v2 package[35,36] for Matlab (Mathworks Inc., Natick, MA, USA). Relationships between craniocaudal CoM position and head, neck, pectoral and pelvic limb first mass moment (all significant relationships in our study, see main text) were tested using REGRESSION's OLS, GLS and OU regression options. No significant deviations from the standard regression results were found, indicating that phylogeny had no significant effect on our analysis.

1.6: Evolutionary Trends in Dorsoventral Centre of Mass Position

Additional analysis of bird-line CoM evolution along the dorso-ventral axis was carried out, although the links of this parameter to terrestrial locomotor biomechanics are less straightforward. The results, shown in Supplementary Figure S1, robustly indicate two evolutionary trends in dorso-ventral CoM position. First, between basal Archosauria and basal Neotheropoda (i.e., in the Triassic period), there was a dramatic (~threefold) dorsal shift (nodes 1-6, Fig. S1). This was followed by a phylogenetically long period of relative stasis until a large ventral shift (~threefold) occurred relatively late in the bird-line, between basal Aves/Avialae and extant Neornithes. Our sensitivity analysis (Fig. S3; see Methods Summary) indicates that these trends are still evident when allowing for considerable variation in the morphological assumptions underlying our reconstruction methodology.

1.5: Alternate Phylogenetic Relationships between *Coelophysis* and *Dilophosaurus*

Some phylogenetic analyses (e.g.[37]) find *Coelophysis* and *Dilophosaurus* as belonging to a discrete basal clade of Neotheropoda, Coelophysoidea (see Figure S2), rather than successive, separate branches as shown in our study's Figure 1. To test whether this alternate relationship structure affects our overall conclusions, our phylogenetic optimisation analysis was repeated

using the phylogeny shown in Figure S2. The results did not show an appreciably different pattern in estimated CoM evolution (Figure S3).

2. Supplementary References

31. Carrano, M.T. Body-size evolution in the Dinosauria. *Amniote Palaeobiology: Perspectives on the Evolution of Mammals, Birds, and Reptiles* (pp. 225–268) (1998).

32. Gatesy, S.M., Middleton, K.M., Jenkins, F.A.J. & Shubin, N.H. Three-dimensional preservation of foot movements in Triassic theropod dinosaurs. *Nature* **810**, 141-144 (1999).

33. Midford, P.E., Garland, T.J. & Maddison, W.P. PDAP package of Mesquite. Version 1.07. (2005).

34. Maddison, W.P. & Maddison, D.R. Mesquite: a modular system for evolutionary analysis. Version 2.75. http://mesquiteproject.org. (2011).

35. Blomberg, S.P., Garland, T. & Ives, A.R. Testing for phylogenetic signal in comparative data: behavioural traits are more labile. *Evolution* **57**, 717-45 (2003).

36. Lavin, S.R., Karasov, W.H., Ives, A.R., Middleton, K.M. & Garland, T. Morphometrics of the avian small intestine compared with that of nonflying mammals: a phylogenetic approach. *Physiological and Biochemical Zoology* **81**, 526-50 (2008).

37. Carrano, M.T., Benson, R.B.J. & Sampson, S.D. The phylogeny of Tetanurae (Dinosauria: Theropoda). *Journal of Systematic Palaeontology* **10**, 211-300 (2012).

38: Benton, M.J. & Donahue, P.C.J. Palaentological evidence to date the tree of life. *Molecular Biology and Evolution* **24**, 26-53. (2007).

39: Sereno, P.C. & Arcucci, A.B. Dinosaurian precursors from the Middle Triassic of Argentina: *Marasuchus lilloensis* gen. nov. *Journal of Vertebrate Paleontology* **14**, 53-73. (1994).

40: Sereno, P.C., Forster, C.A., Rogers, R.R., & Monetta, A.M. Primitive dinosaur skeleton from Argentina and the early evolution of Dinosauria. *Nature* **361**, 64-66. (1993).

41: Cope, E.D. On a new genus of Triassic Dinosauria. *American Naturalist* **XXII**: 626. (1889).

42: Yates, A.M. A new theropod dinosaur from the Early Jurassic of South Africa and its implications for the early evolution of theropods. *Palaeontological Africana* **41**, 105-122. (2006).

43: Currie, P.J. & Zhao, X.J. A new carnosaur *(Dinosauria, Theropoda)* from the Jurassic of Xinjiang, People's Republic of China. *Canadian Journal of Earth Sciences* **30**, 2037-2081. (1994).

44: Xu, X. & Zhang, F.A new maniraptoran dinosaur from China with long feathers on the metatarsus. *Naturwissenschaften* **92**, 173-177. (2005).

45: Hu, D., Zhang, L. & Xu, X. A pre-*Archaeopteryx* troodontid theropod from China with long feathers on the metatarsus. *Nature* **461**, 640-643. (2009).

46: von Meyer, H. *Archaeopteryx lithographica* (Vogel-Feuder) und Pterodactylys von Solenhofen. *Neues Jahrbuch f*ür *Mineralogie, Geognosie, Geologie und Petrefakten-Kunde* **1861**, 678-679. (1861).

47: Zhang, F. & Zhou, Z. A primitive enantiornithine bird and the origin of feathers. *Science* **290**, 1955-1959. (2000).

48: Zhou, Z. & Zhang, F. Two new ornithurine birds from the Early Cretaceous of western Liaoning, China. *Chinese Science Bulletin* **46**, 1258-1264. (2001).

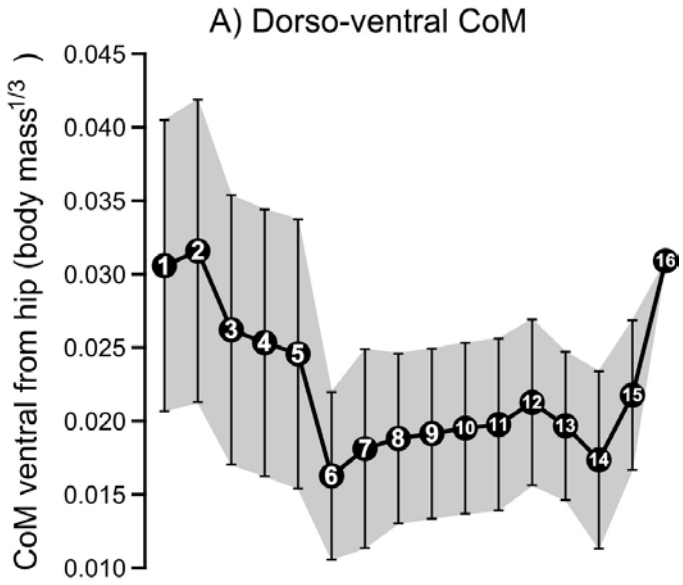

Figure S1: Estimated evolutionary trends (numbers 1-16 are for nodes in Figure 1) in centre of mass (CoM) position in units of mean estimated body mass$^{1/3}$, along the dorso-ventral axis. Whisker-plot bars represent the range of values indicated by our sensitivity analysis. Values toward the extreme ends of the whisker plots are less plausible (maximal/minimal models with extreme proportions) whereas values toward the middle are more plausible, conservatively proportioned models.

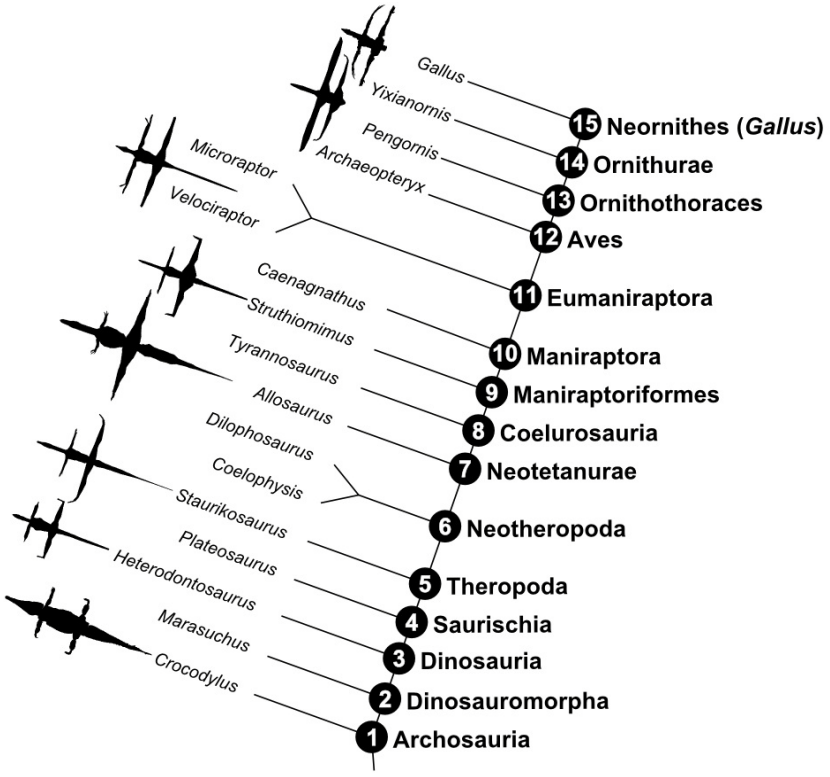

Figure S2: Alternative phylogeny to that shown in Figure 1: *Coelophysis* and *Dilophosaurus* form a discrete clade (Coelophysoidea) of basal Neotheropoda.

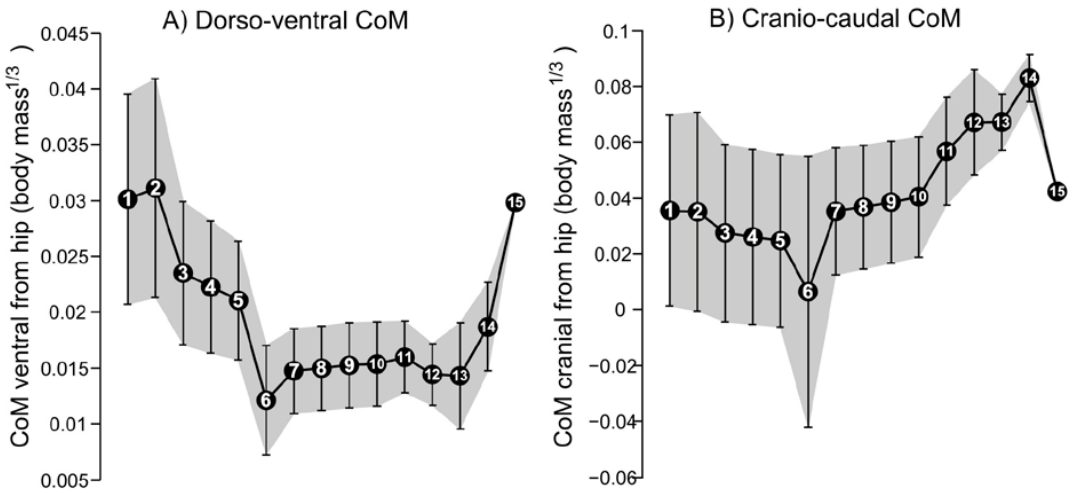

Figure S3: Estimated evolutionary trends (numbers 1-15 are for nodes in Figure S1) in centre of mass (CoM) position (in units of mean estimated body mass$^{1/3}$), along dorso-ventral (**a**) and craniocaudal (**b**) axes, using the alternate phylogeny shown in Figure S2. As in Figure 3, whisker-plot bars represent the range of values indicated by our sensitivity analysis.

4. Supplementary Tables

Table S1: Study specimen information, indicating completeness of specimen and methods used to reconstruct or estimate the dimensions of missing elements.

Taxa	Specimen Number	Institution	Scanning Method	Completeness	Reconstruction Method
Crocodylus johnstoni	n/a	RVC (only scan remains)	CT	Complete	Whole cadaveric subadult specimen
Marasuchus lilloensis	BMNH R14101	Natural History Museum, UK	Laser Surface Scan	Ribcage Missing	Chest cavity assumed to be roughly ellipsoid, fitted to available landmarks: Pelvic depth, Width of pectoral girdle, curvature of dorsal vertebrae
Heterodontosaurus tucki	12916	UCMP Berkeley	Laser Surface Scan	Partial Ribcage Only	Chest reconstructed by fitting ellipsoid hoops to available ribs and other landmarks (as above)
Staurikosaurus pricei	MCZ 1669	Museum of Comparative Zoology, Harvard	Laser Surface Scan	Complete Sculpt	Sculpted reconstruction by Orlando Grillo, based on type specimen MCZ 1669
Plateosaurus engelhardti	GPIT1 & GPIT2	Eberhardt-Karls-Universitat Tubingen	Laser and Tactile Surface Scan	Near Complete	Mostly GPIT1, some scaled elements from GPIT2 used, assembled by Heinrich Mallison (Humboldt MFN)
Coelophysis bauri	10971 (Composite Mount)	Cleveland Museum of Natural History	Laser Surface Scan	Complete*	Some (minor) elements sculpted when cast originally reconstructed
Dilophosaurus wetherilli	37302	UCMP Berkeley	Laser Surface Scan	Ribcage Missing, Pubis Fragmented	Chest section scaled from *Coelophysis*, fitted to pelvic and pectoral girdles, dorsal vertebrae. Pubis reconstructed according to Welles 1954
Allosaurus fragilis	SMA 0005	Sauriermuseum, Aathal	Laser Surface Scan	Complete	Some (minor) elements sculpted when cast originally reconstructed
Tyrannosaurus rex	CM 9380	Carnegie Museum of Natural History, Pittsburgh	Laser Surface Scan	Partial skeleton	Many elements sculpted when cast originally reconstructed but proportions similar to other, more complete specimens
Struthiomimus sedens	BHI 1266	Black Hills Institute	Laser Surface Scan	Near Complete	Some (minor) elements sculpted when cast originally reconstructed. Scanned by Karl T. Bates.
cf. Caenagnathus	CM78001	Carnegie Museum of Natural History, Pittsburgh	Digital Model	Complete	Digitally sculpted reconstruction by Jason Adam Bannister (Mechanimal), from measurements of actual skeleton
Microraptor gui	IVPP V13352	Institute of Vertebrae Palaeontology and Palaeoanthropology, Beijing	CT	Complete Sculpt	Sculpted reconstruction by Jason Brougham (AMNH) based on holotype IVPP V13352 MCZ 1669
Velociraptor mongoliensis	IGM 100/986 & 987	IGM, Ulaan Baatar	Laser Surface Scan	Partial Ribcage Only	Chest section scaled from *Archaeopteryx*, fitted to pelvic and pectoral girdles, dorsal vertebrae.
Archaeopteryx lithographica	HMN 1880	Humboldt MFN	Laser Surface Scan	Complete Sculpt	Sculpted reconstruction by Janice Hertel, based on specimen HMN 1880

Pengornis houi	IVPP V15336	Institute of Vertebrate Palaeontology and Palaeoanthropology, Beijing	μCT	Ribcage Missing, Skull Compacted	Chest section scaled from *Yixianornis*, fitted to pelvic and pectoral girdles, dorsal vertebrae. Skull scaled from *Archaeopteryx* to fit visible landmarks on compacted skull.
Yixianornis grabaui	IVPP V12558	Institute of Vertebrae Palaeontology and Palaeoanthropology, Beijing	μCT	Skull Compacted	Skull scaled from *Archaeopteryx* to fit visible landmarks on compacted skull.
Gallus gallus (Red Junglefowl)	n/a	RVC (only scan remains)	CT	Complete	Whole cadaveric adult specimen

Table S2: Phylogenetic nodes used in phylogenetic optimisation analysis (ancestral state estimation). Ages shown in Ma (millions of years) are approximate estimated age of splitting events defined by node, based on information from the references indicated in the Sources column (see Supplementary References).

Node	Date (Ma)	Stage	Sources
Archosauria	246.5	Anisian / Olanakian	Benton & Donahue 2007[38]
Dinosauromorpha	237	Anisian / Ladinian	Age of *Marasuchus lilloensis*[39], plus 1ma
Dinosauria	231	Early Carnian	Age of *Eoraptor lunensis*[40] plus 3ma
Saurischia	230	Early Carnian	Age of *Eoraptor lunensis*[40] plus 2ma
Theropoda	229	Early Carnian	Age of *Eoraptor lunensis*[40] plus 1ma
Neotheropoda	217	Carnian / Norian	Age of *Coelophysis bauri*[41] plus 1ma
Tetanurae	196	Sinemurian	Age of *Dracovenator regenti*[42] plus 1ma
Neotetanurae	167	Bathonian	Age of *Sinraptor dongi*[43] plus 1ma
Coelurosauria	166	Callovian	Age of *Pedopenna daohugouensis*[44] plus 3ma
Maniraptoriformes	165	Callovian	Age of *Pedopenna daohugouensis*[44] plus 2ma
Maniraptora	164	Callovian	Age of *Pedopenna daohugouensis*[44] plus 1ma
Eumaniraptora	156	Oxfordian / Kimmeridgian	Age of *Anchiornis huxleyi*[45] plus 1ma
Aves/Avialae	152	Kimmeridgian / Tithonian	Age of *Archaeopteryx lithographica*[46] plus 1ma
Ornithothoraces	128.5	Barremian	Age of *Protopteryx fengningensis*[47] plus 1ma
Ornithurae	122	Bathonian	Age of *Yixianornis grabaui*[48] plus 1ma
Neornithes (*Gallus*)	Present	n/a	n/a

Table S3: Lengths of individual modelled body segments for each specimen, in metres.

Taxa	Gleno-Acetabular Length (m)	Tail Length (m)	Pectoral Limb Length (m)	Pelvic Limb Length (m)	Femur Length (m)
Crocodylus johnstoni	0.421	0.878	0.253	0.264	0.099
Marasuchus lilloensis	0.115	0.262	0.103	0.161	0.047
Heterodontosaurus tucki	0.240	0.576	0.187	0.313	0.094
Staurikosaurus pricei	0.348	1.320	0.299	0.602	0.198
Plateosaurus engelhardti	1.300	2.820	0.816	1.300	0.488
Coelophysis bauri	0.423	1.510	0.232	0.488	0.151
Dilophosaurus wetherilli	1.290	3.150	0.713	1.450	0.480
Allosaurus fragilis	1.240	4.140	0.721	1.810	0.644
Tyrannosaurus rex	1.820	7.600	0.873	3.040	1.040
Struthiomimus sedens	1.170	2.910	1.050	1.730	0.545
cf. Caenagnathus	0.246	0.431	0.351	0.539	0.170
Velociraptor mongoliensis	0.290	0.626	0.437	0.486	0.163
Microraptor gui	0.127	0.491	0.223	0.285	0.087
Archaeopteryx lithographica	0.065	0.134	0.133	0.103	0.036
Pengornis houi	0.056	0.030	0.177	0.117	0.044
Yixianornis grabaui	0.064	0.021	0.155	0.119	0.036
Gallus gallus (Red Junglefowl)	0.136	0.099	0.234	0.334	0.087

Table S4: Estimated masses of individual modelled body segments for each specimen in kilograms, showing maximal, minimal and mean iterations of modelled volumes. Segment volumes for extant taxa (*Crocodylus johnstoni* and *Gallus gallus*) were taken directly from CT data without iteration[18], and so only the values for these 'real' segment volumes are shown (in the 'mean values' columns). (note: pelvic and pectoral limb masses are counted twice when calculating whole body mass).

Taxa	Max Whole-Body Mass (kg)	Min Whole-Body Mass (kg)	Mean Whole-Body Mass (kg)	Head Mass (kg)	Max Neck Mass (kg)	Min Neck Mass (kg)	Mean Neck Mass (kg)	Max Trunk Mass (kg)	Min Trunk Mass (kg)	Mean Trunk Mass (kg)
Crocodylus johnstoni	-	-	20.9	1.19	-	-	1.89	-	-	10.5
Marasuchus lilloensis	0.382	0.194	0.288	0.00636	0.0179	0.00488	0.0114	0.172	0.0958	0.134
Heterodontosaurus tucki	5.99	3.02	4.50	0.191	0.413	0.155	0.284	3.22	1.59	2.40
Staurikosaurus pricei	28.3	14.2	21.3	0.662	1.93	0.596	1.264	11.0	5.99	8.48
Plateosaurus engelhardti	1020	484	753	3.77	30.3	13.3	21.8	528	259	394
Coelophysis bauri	24.9	11.7	18.3	0.453	2.25	0.617	1.43	11.4	5.83	8.48
Dilophosaurus wetherilli	625	298	462	12.5	55.0	15.4	35.2	323	165	244
Allosaurus fragilis	1880	895	1340	28.9	119	54.7	86.9	806	385	596
Tyrannosaurus rex	14000	7500	10800	382	728	375	551	8400	4270	6340
Struthiomimus sedens	741	394	568	1.89	25.6	12.0	18.8	313	189	251
cf. Caenagnathus	15.7	9.34	12.5	0.256	0.972	0.314	0.643	6.28	3.39	4.84
Velociraptor mongoliensis	18.3	9.89	14.1	0.458	2.12	0.581	1.35	6.45	3.88	5.17
Microraptor gui	1.59	0.832	1.21	0.0219	0.0591	0.0283	0.0437	0.742	0.357	0.549
Archaeopteryx lithographica	0.132	0.0663	0.0992	0.00455	0.0135	0.00378	0.00862	0.0670	0.0321	0.0495
Pengornis houi	0.311	0.159	0.229	0.00672	0.0214	0.00670	0.0140	0.106	0.0613	0.0835
Yixianornis grabaui	0.266	0.136	0.201	0.0108	0.0284	0.00757	0.0180	0.124	0.0576	0.0910
Gallus gallus (Red Junglefowl)	-	-	2.57	0.0739	-	-	0.151	-	-	0.875

Table S4 continued

Taxa	Max Tail Mass (kg)	Min Tail Mass (kg)	Mean Tail Mass (kg)	CFL Muscle Mass (kg)	Max Pectoral Limb Mass (kg)	Min Pectoral Limb Mass (kg)	Mean Pectoral Limb Mass (kg)	Max Pelvic Limb Mass (kg)	Min Pelvic Limb Mass (kg)	Mean Pelvic Limb Mass (kg)
Crocodylus johnstoni	-	-	4.98	0.356	-	-	0.408	-	-	0.722
Marasuchus lilloensis	0.0742	0.0258	0.0500	0.00260	0.0120	0.00702	0.00950	0.0440	0.0237	0.0339
Heterodontosaurus tucki	0.999	0.393	0.696	0.0224	0.139	0.104	0.122	0.445	0.242	0.344
Staurikosaurus pricei	5.56	1.89	3.73	0.419	0.548	0.358	0.453	4.09	2.16	3.12
Plateosaurus engelhardti	215	74.1	144	0.0458	20.2	13.4	16.8	102	53.6	78.0
Coelophysis bauri	6.33	2.37	4.35	0.541	0.245	0.190	0.218	2.04	1.03	1.53
Dilophosaurus wetherilli	100	34.9	67.5	7.24	6.58	4.40	5.49	60.8	31.1	46.0
Allosaurus fragilis	334	157	245	32.7	18.1	13.3	15.7	226	121	173
Tyrannosaurus rex	2070	1010	1540	191	53.0	45.7	49.4	1160	684	920
Struthiomimus sedens	88.3	31.4	59.9	6.31	11.5	7.32	9.39	145	72.6	109
cf. *Caenagnathus*	1.23	0.492	0.863	0.121	0.503	0.359	0.431	3.00	2.08	2.54
Velociraptor mongoliensis	2.78	1.26	2.02	0.122	0.633	0.392	0.513	2.64	1.46	2.05
Microraptor gui	0.149	0.0797	0.114	N/A	0.105	0.0645	0.0847	0.204	0.108	0.156
Archaeopteryx lithographica	0.0102	0.00457	0.00740	0.000452	0.00720	0.00461	0.00591	0.00112	0.00601	0.00862
Pengornis houi	0.00438	0.00402	0.00420	0.000116	0.0502	0.0238	0.0370	0.0301	0.0161	0.0231
Yixianornis grabaui	0.00165	0.000805	0.00123	0.0000504	0.0343	0.0215	0.0279	0.0163	0.00801	0.0121
Gallus gallus (Red Junglefowl)	-	-	0.076	0.00154	-	-	0.333	-	-	0.363

Table S5: Estimated CoM positions of individual modelled body segments for each specimen, showing estimated position along the craniocaudal axis for the mean mass iteration of each segment only (see Table S4), in metres cranial to the hip joint.

Taxa	Head CoM (m)	Mean Craniocaudal Neck CoM (m)	Mean Craniocaudal Trunk CoM (m)	Mean Craniocaudal Tail CoM (m)	Mean Craniocaudal Pectoral Limb CoM (m)	Mean Craniocaudal Pelvic Limb CoM (m)
Crocodylus johnstoni	0.667	0.518	0.192	-0.263	0.43	0.0000399
Marasuchus lilloensis	0.159	0.136	0.0562	-0.086	0.119	-0.00235
Heterodontosaurus tucki	0.316	0.263	0.0998	-0.225	0.237	-0.00421
Staurikosaurus pricei	1.94	1.55	0.588	-0.884	1.19	-0.0262
Plateosaurus engelhardti	0.597	0.458	0.163	-0.321	0.35	-0.0027
Coelophysis bauri	0.692	0.548	0.213	-0.364	0.416	-0.0136
Dilophosaurus wetherilli	1.99	1.59	0.7	-0.875	1.26	-0.003
Allosaurus fragilis	1.97	1.51	0.623	-1.2	1.18	-0.0222
Tyrannosaurus rex	3.74	2.84	0.93	-2.42	2.26	-0.0455
Struthiomimus sedens	1.67	1.28	0.392	-0.959	0.978	-0.00915
cf. Caenagnathus	0.428	0.294	0.11	-0.166	0.238	-0.000762
Velociraptor mongoliensis	0.501	0.359	0.0974	-0.206	0.291	-0.00368
Microraptor gui	0.189	0.151	0.066	-0.139	0.124	-0.000175
Archaeopteryx lithographica	0.104	0.0817	0.0374	-0.0472	0.0635	0.000697
Pengornis houi	0.112	0.0745	0.02	-0.0233	0.0504	0.00287
Yixianornis grabaui	0.118	0.0918	0.0403	-0.0159	0.073	0.000232
Gallus gallus (Red Junglefowl)	0.226	0.173	0.0534	-0.0609	0.124	-0.00122

Table S6: Estimated First Mass Moments (mean mass [Table S5] multiplied by CoM position [Table S6]) of individual modelled segments for each taxa, shown in kilogram metres. Values are defined about the hip, and so positive values represent a cranial moment and negative values a caudal moment.

Taxa	Head Cranio-Caudal First Mass Moment (kg m)	Neck Cranio-Caudal First Mass Moment (kg m)	Trunk Cranio-Caudal First Mass Moment (kg m)	Tail Cranio-Caudal First Mass Moment (kg m)	Pectoral Limb Cranio-Caudal First Mass Moment (kg m)	Pelvic Limb Cranio-Caudal First Mass Moment (kg m)
Crocodylus johnstoni	0.793	0.979	2.03	-1.31	0.176	0.0000288
Marasuchus lilloensis	0.00101	0.00155	0.00752	-0.00429	0.00113	-0.0000795
Heterodontosaurus tucki	0.0605	0.0746	0.24	-0.157	0.0289	-0.00145
Staurikosaurus pricei	7.32	33.9	231	-128	20	-2.04
Plateosaurus engelhardti	0.395	0.579	1.38	-1.2	0.159	-0.00845
Coelophysis bauri	0.314	0.784	1.83	-1.58	0.0905	-0.0208
Dilophosaurus wetherilli	24.8	56.1	171	-59.1	6.9	-0.138
Allosaurus fragilis	56.8	131	371	-296	18.6	-3.85
Tyrannosaurus rex	1430	1570	5890	-3730	112	-41.9
Struthiomimus sedens	3.16	24.1	98.4	-57.4	9.18	-0.993
cf. Caenagnathus	0.109	0.189	0.53	-0.143	0.102	-0.00193
Velociraptor mongoliensis	0.229	0.484	0.503	-0.416	0.149	-0.00755
Microraptor gui	0.00414	0.00662	0.0363	-0.0159	0.0105	-0.0000272
Archaeopteryx lithographica	0.000475	0.000704	0.00185	-0.000349	0.000375	0.00000601
Pengornis houi	0.000754	0.00105	0.00167	-0.0000977	0.00187	0.0000663
Yixianornis grabaui	0.00128	0.00165	0.00366	-0.0000195	0.00204	0.00000282
Gallus gallus (Red Junglefowl)	0.0167	0.0261	0.0467	-0.0046	0.0413	-0.000443

Table S7: Estimated CoM positions for individual specimens, showing maximal, minimal and mean estimated position along the craniocaudal and dorsoventral axes, in metres cranial or ventral from the hip joint. As whole-body volumes for extant taxa (*Crocodylus johnstoni* and *Gallus gallus*) were taken directly from CT data without iteration[18], only values for the 'real' body volumes are shown (in the 'mean values' columns).

Taxa	Maximally Cranial CoM (m)	Maximally Caudal CoM (m)	Mean Craniocaudal CoM (m)	Maximally Dorsal CoM (m)	Maximally Ventral CoM (m)	Mean Dorsoventral CoM (m)
Crocodylus johnstoni	-	-	0.136	-	-	0.0128
Marasuchus lilloensis	0.0493	0.00523	0.0273	0.0147	0.0285	0.0215
Heterodontosaurus tucki	0.102	0.0113	0.0565	0.0331	0.0508	0.0420
Staurikosaurus pricei	0.145	-0.00312	0.0711	0.159	0.250	0.205
Plateosaurus engelhardti	0.480	-0.00485	0.238	0.0391	0.0959	0.0675
Coelophysis bauri	0.185	-0.0288	0.0782	0.0267	0.0550	0.0408
Dilophosaurus wetherilli	0.676	0.185	0.430	0.0867	0.201	0.144
Allosaurus fragilis	0.456	-0.0216	0.217	0.0956	0.210	0.153
Tyrannosaurus rex	0.814	0.112	0.463	0.284	0.401	0.343
Struthiomimus sedens	0.311	0.00974	0.161	0.210	0.304	0.257
cf. *Caenagnathus*	0.102	0.0389	0.0704	0.0331	0.0870	0.0601
Velociraptor mongoliensis	0.128	0.0251	0.0763	0.0431	0.0852	0.0641
Microraptor gui	0.0604	0.0209	0.0406	0.0362	0.0579	0.0471
Archaeopteryx lithographica	0.0427	0.0240	0.0334	0.00672	0.0112	0.00897
Pengornis houi	0.0366	0.0252	0.0309	0.00248	0.0116	0.00704
Yixianornis grabaui	0.0568	0.0476	0.0522	0.0102	0.0160	0.0131
Gallus gallus (Red Junglefowl)	-	-	0.0649	-	-	0.0423

Table S8: Estimated CoM positions at phylogenetic nodes, with values for *Gallus gallus* (values from Table S5, in units of body mass$^{1/3}$ cranial to the hip) inserted to represent Neornithes. As in Table S7, values for maximal, minimal and mean estimated CoM position are shown, in units of mean body mass$^{1/3}$ (linearised body mass) cranially from the hip joint.

Node	Maximally Cranial CoM (body mass$^{1/3}$ cranial from hip)	Maximally Caudal CoM (body mass$^{1/3}$ cranial from hip)	Mean Craniocaudal CoM (body mass$^{1/3}$ cranial from hip)
Archosauria	0.0720	0.00875	0.0404
Dinosauromorpha	0.0728	0.00718	0.0400
Dinosauria	0.0624	0.00176	0.0321
Saurischia	0.0607	0.000710	0.0307
Theropoda	0.0593	-0.000291	0.0295
Neotheropoda	0.0698	-0.00898	0.0304
Tetanurae	0.0801	0.0163	0.0482
Neotetanurae	0.0638	0.0195	0.0416
Coelurosauria	0.0646	0.0210	0.0428
Maniraptoriformes	0.0657	0.0226	0.0442
Maniraptora	0.0671	0.0244	0.0458
Eumaniraptora	0.0802	0.0397	0.0600
Aves/Avialae	0.0895	0.0498	0.0697
Ornithothoraces	0.0798	0.0595	0.0697
Ornithurae	0.0943	0.0781	0.0862
Neornithes (*Gallus*)	0.0474	0.0474	0.0474

Table S9: Mean estimated body segment masses (in units of mean body mass) at phylogenetic nodes, with values for *Gallus gallus* (values from Table S4) inserted to represent Neornithes. Values shown are Mesquite outputs based on mean segment masses (Table S4) normalised by dividing by mean whole-body mass (Table S4).

Node	Head Mass (body mass)	Mean Neck Mass (body mass)	Mean Trunk Mass (body mass)	Mean Tail Mass (body mass)	Mean Pectoral Limb Mass (body mass)	Mean Pelvic Limb Mass (body mass)	CFL Muscle Mass (body mass)
Archosauria	0.0241	0.0434	0.463	0.177	0.0313	0.115	0.000323
Dinosauromorpha	0.0228	0.0416	0.462	0.175	0.0318	0.118	0.000926
Dinosauria	0.0264	0.0527	0.446	0.180	0.0248	0.123	0.00454
Saurischia	0.0266	0.0542	0.441	0.182	0.0236	0.125	0.00703
Theropoda	0.0276	0.0568	0.4322	0.183	0.0224	0.128	0.0119
Neotheropoda	0.0250	0.0764	0.468	0.230	0.0128	0.0875	0.0125
Tetanurae	0.0269	0.0753	0.507	0.162	0.0149	0.0993	0.0132
Neotetanurae	0.0296	0.0697	0.477	0.133	0.0304	0.115	0.0138
Coelurosauria	0.0300	0.0698	0.477	0.129	0.0321	0.115	0.0166
Maniraptoriformes	0.0306	0.0701	0.477	0.125	0.0341	0.115	0.0253
Maniraptora	0.0313	0.0707	0.4775	0.121	0.0363	0.114	0.00649
Eumaniraptora	0.0386	0.0775	0.485	0.0917	0.0537	0.0999	0.00706
Aves/Avialae	0.0444	0.0848	0.494	0.0761	0.0610	0.0893	0.00719
Ornithothoraces	0.0419	0.0766	0.420	0.0211	0.138	0.0821	0.00842
Ornithurae	0.0521	0.0875	0.447	0.00825	0.139	0.0639	0.00872
Neornithes (*Gallus*)	0.0288	0.0589	0.341	0.0294	0.130	0.142	0.000523

Table S10: Estimated body segment craniocaudal CoM positions (in units of mean body mass$^{1/3}$ cranial to the hip) at phylogenetic nodes, with values for *Gallus gallus* (values from Table S4) inserted to represent Neornithes. Values shown are Mesquite outputs based on CoMs for mean mass segment iterations (Table S6) normalised by dividing by mean whole-body mass$^{1/3}$ (Table S4).

Node	Head Cranio-Caudal CoM (body mass$^{1/3}$)	Neck Cranio-Caudal CoM (body mass$^{1/3}$)	Trunk Cranio-Caudal CoM (body mass$^{1/3}$)	Tail Cranio-Caudal CoM (body mass$^{1/3}$)	Pectoral Limb Cranio-Caudal CoM (body mass$^{1/3}$)	Pelvic Limb Cranio-Caudal CoM (body mass$^{1/3}$)
Archosauria	0.239	0.207	0.0825	-0.128	0.175	-0.00326
Dinosauromorpha	0.239	0.202	0.0830	-0.129	0.175	-0.00339
Dinosauria	0.227	0.183	0.0704	-0.123	0.149	-0.00248
Saurischia	0.226	0.181	0.0686	-0.121	0.145	-0.00233
Theropoda	0.225	0.178	0.0670	-0.121	0.141	-0.00215
Neotheropoda	0.260	0.205	0.0800	-0.136	0.156	-0.00476
Tetanurae	0.250	0.199	0.0847	-0.117	0.156	-0.00136
Neotetanurae	0.206	0.160	0.0673	-0.107	0.125	-0.000666
Coelurosauria	0.207	0.160	0.0673	-0.107	0.125	-0.000558
Maniraptoriformes	0.207	0.161	0.0676	-0.106	0.125	-0.000434
Maniraptora	0.208	0.161	0.0682	-0.106	0.126	-0.000304
Eumaniraptora	0.215	0.168	0.0740	-0.104	0.131	0.000739
Aves/Avialae	0.222	0.174	0.0787	-0.100	0.135	0.00139
Ornithothoraces	0.197	0.144	0.0545	-0.0420	0.108	0.00238
Ornithurae	0.201	0.155	0.0667	-0.0292	0.122	0.000651
Neornithes (*Gallus*)	0.165	0.126	0.0390	-0.0445	0.0907	-0.000890

Table S11: Mean estimated body segment craniocaudal first mass moments (mass * CoM position, in units of mean body mass$^{4/3}$) at phylogenetic nodes, with values for *Gallus gallus* (values from Table S4) inserted to represent Neornithes. Values are defined about the hip, and so positive values represent a cranial moment and negative values a caudal moment. Values shown are Mesquite outputs based on multiplying mean segment masses (normalised by dividing by mean whole-body mass) and mean segment CoMs (normalised by dividing by mean whole body mass$^{1/3}$ - all from Table S4)

Node	Head Cranio-Caudal First Mass Moment (body mass$^{4/3}$)	Neck Cranio-Caudal First Mass Moment (body mass$^{4/3}$)	Trunk Cranio-Caudal First Mass Moment (body mass$^{4/3}$)	Tail Cranio-Caudal First Mass Moment (body mass$^{4/3}$)	Pectoral Limb Cranio-Caudal First Mass Moment (body mass$^{4/3}$)	Pelvic Limb Cranio-Caudal First Mass Moment (body mass$^{4/3}$)
Archosauria	0.00575	0.00869	0.0386	-0.0225	0.00552	-0.000382
Dinosauromorpha	0.00544	0.00836	0.0384	-0.0225	0.00561	-0.000396
Dinosauria	0.00593	0.00956	0.0316	-0.0222	0.00381	-0.000277
Saurischia	0.00595	0.00974	0.0305	-0.0221	0.00350	-0.000260
Theropoda	0.00616	0.0101	0.0292	-0.0222	0.00322	-0.000241
Neotheropoda	0.00648	0.0157	0.0374	-0.0314	0.00199	-0.000403
Tetanurae	0.00673	0.0151	0.0433	-0.0194	0.00225	-0.000124
Neotetanurae	0.00623	0.0114	0.0324	-0.0147	0.00391	-0.0000956
Coelurosauria	0.00636	0.0115	0.0325	-0.0142	0.00413	-0.0000842
Maniraptoriformes	0.00650	0.0115	0.0326	-0.0137	0.00439	-0.0000719
Maniraptora	0.00669	0.0117	0.0329	-0.0132	0.00467	-0.0000582
Eumaniraptora	0.00848	0.0132	0.0362	-0.00979	0.00704	0.0000522
Aves/Avialae	0.00992	0.0148	0.0391	-0.007824	0.00816	0.000119
Ornithothoraces	0.00836	0.0113	0.0239	-0.00145	0.0143	0.000231
Ornithurae	0.0105	0.0136	0.0300	-0.000344	0.0169	0.0000503
Neornithes (*Gallus*)	0.00476	0.00743	0.0133	-0.00131	0.0118	-0.000126

Table S12: Correlation results (Spearman's Rank, see Methods Summary) for mean estimated craniocaudal CoM position *vs*. all study variables, including segment masses. Positive R values indicate that larger variables are associated with a more cranial CoM and vice versa. Bracketed values after variable name indicate nodes excluded as outliers (>2 S.D. from mean).

Variable (Excluded Nodes)	Spearman's R	Spearman's P
Head Mass (16)	0.45	0.08
Neck Mean Mass (16)	0.41	0.11
Trunk Mean Mass (16)	0.01	0.96
Tail Mean Mass (16)	-0.32	0.23
Pectoral Limb Mean Mass (15,16)	0.51	0.05
Pelvic Limb Mean Mass (11,16)	-0.41	0.12
Head CoM X (16)	0.26	0.34
Neck Mean CoM X (16)	0.18	0.51
Trunk Mean CoM X (16)	0.31	0.25
Tail Mean CoM X (16)	0.27	0.31
Pectoral Limb Mean CoM X (16)	0.24	0.38
Pelvic Limb Mean CoM X (15,16)	0.50	0.06
Caudofemoralis Mass (6,16)	-0.37	0.20
Head X Moment (1,16)	0.47	0.08
Neck Mean X Moment (16)	0.44	0.08
Trunk Mean X Moment (16)	0.30	0.25
Tail Mean X Moment (6,16)	0.17	0.53
Pectoral Limb Mean X Moment (16)	0.67	0.00
Pelvic Limb Mean X Moment (15,16)	0.58	0.02